Demonstration of 3 kW-Level Nearly Single Mode Monolithic Fiber Amplifier Emitting at 1050 Nm Employing Tapered Yb-Doped Fiber

Xiangming Meng, Yun Ye, Baolai Yang, Xiaoming Xi, Peng Wang, Chen Shi, Zhiyong Pan, Liangjin Huang, Hanwei Zhang, and Xiaolin Wang

***Abstract*—Tapered Yb-doped fiber (T-YDF) can balance the suppression of transverse mode instability (TMI) and stimulated Raman scattering (SRS) in high power fiber lasers. In this work, we have constructed an all-fiberized master oscillator power amplifier emitting at the central wavelength of 1050 nm based on a T-YDF and investigated the laser performance in respective co-pumped and counter-pumped configurations. The results show that the T-YDF can effectively mitigate SRS effect in short-wavelength fiber lasers. A nearly single mode beam quality (M2∼1.20) is obtained at output power of 3 kW-level. In particular, the SRS suppression ratio in the co-pump and counter-pump scheme is about ∼33.2 dB at ∼3039 W and ∼46.6 dB at ∼2818 W, respectively. By further optimizing the structure of the tapered active fiber, it is promising to further improve the output power and beam quality in short-wavelength fiber lasers.**

***Index Terms*—High power, short-wavelength fiber lasers, stimulated Raman scattering, tapered Yb-doped fiber, transverse mode instability.**

I. Introduction

HIGH-POWER short-wavelength fiber lasers have important applications in the field of spectral combining and nonlinear frequency conversion [1], [2]. The spectral combining technology based on dispersive element can improve output power while maintaining the beam quality. This technology uses dichroic mirrors to combine multiple lasers operating at different wavelengths through transmission and reflection, which also puts forward a demand for high-power short-wavelength and long-wavelength lasers [3], [4]. There has been reports on high-power short-wavelength fiber lasers in the last decade [5], [6], [7], [8], [9]. In 2016, Naderi et al. reported a fiber laser based on phase- modulated single-frequency laser [5]. The fiber amplifier achieved a 1 kW output at 1030 nm. In 2021, Xu et al. demonstrated a fiber laser emitting at 1045 nm with an output power of 2.4 kW [8]. They adopted 8.5-m-long gain fiber for suppressing the amplified spontaneous emission (ASE) effect. In 2022, Zheng et al. realized a fiber laser operating at 1050 nm with pump-sharing oscillator-amplifier structure [9]. The fiber laser delivered 3.1 kW output power. If methods such as optimizing fiber length are used to suppress ASE, nonlinear effects such as stimulated Raman scattering (SRS) will be the main problem in short-wavelength fiber amplifier.

In 2008, researchers from Tampere University of Technology in Finland reported a fiber laser based on a tapered double-clad fiber and realized a single mode output power of 84 W [10]. Since then, the tapered Yb-doped fiber (T-YDF) with a longitudinally varying core diameter has been developed and extensively applied in high-power lasers fields [11], [12], [13], [14], [15], [16], [17], [18], [19], [20], [21], [22]. The T-YDF can control the number of supported modes in the small-core section, which can improve laser beam quality and mitigate the transverse mode instability (TMI) [11], [12], [13]. The large-core section can suppress the intensity of nonlinear effects, such as SRS [14], [15]. Thanks to the nonuniform longitudinal geometry, the tapered fiber itself also has strong ASE suppression capability [10], [16], [17]. In 2018, Fedotov et al. applied a tapered fiber with a core diameter of 96 μm to construct a 1040 nm linearly polarized continuous wave (CW) laser with an output power of 70 W [18]. In 2019, our research group presented fiber oscillators and fiber amplifiers based on tapered double-clad fibers, which has a narrow end of ∼20/400 μm and a wide end of ∼30/600 μm [11], [19]. The fiber oscillators and fiber amplifiers achieved a maximum output power of 1350 W and 2170 W at 1080 nm, respectively. In 2022, Ye et al. fabricated a large-mode-area (LMA) step-index constant-cladding tapered-core YDF with a cladding diameter of ∼600 μm and reported a 2.49 kW fiber laser at 1080 nm [20]. Most of the reported tapered fiber lasers/amplifiers are centered around 1070–1080 nm and few research was demonstrated in short-wavelength high-power fiber lasers. Benefiting

Manuscript received 3 April 2023; revised 5 May 2023; accepted 15 May 2023. Date of publication 17 May 2023; date of current version 16 June 2023. This work was supported in part by the Open Research Fund of State Key Laboratory of Pulsed Power Laser Technology, Electronic Countermeasure Institute, National University of Defense Technology under Grant SKL2022ZR02 and in part by the National Natural Science Foundation of China under Grant 62005315. *(Corresponding authors: Baolai Yang; Xiaolin Wang.)*

Xiangming Meng and Yun Ye are with the College of Advanced Interdisciplinary Studies, National University of Defense Technology, Changsha 410073, China (e-mail: mxm_er@163.com; yeyun2015@163.com).

Baolai Yang, Xiaoming Xi, Peng Wang, Chen Shi, Zhiyong Pan, Liangjin Huang, Hanwei Zhang, and Xiaolin Wang are with the College of Advanced Interdisciplinary Studies, National University of Defense Technology, Changsha 410073, China, also with the Nanhu Laser Laboratory, National University of Defense Technology, Changsha 410073, China, and also with the Hunan Provincial Key Laboratory of High Energy Laser Technology, National University of Defense Technology, Changsha 410073, China (e-mail: yangbaolai1989@163.com; exixiaoming@163.com; 1169723259@qq.com; bigbryant@nudt.edu.cn; panzy168@163.com; hlj203@nudt.edu.cn; zhanghanwei100@163.com; chinawxllin@163.com).

Digital Object Identifier 10.1109/JPHOT.2023.3277201

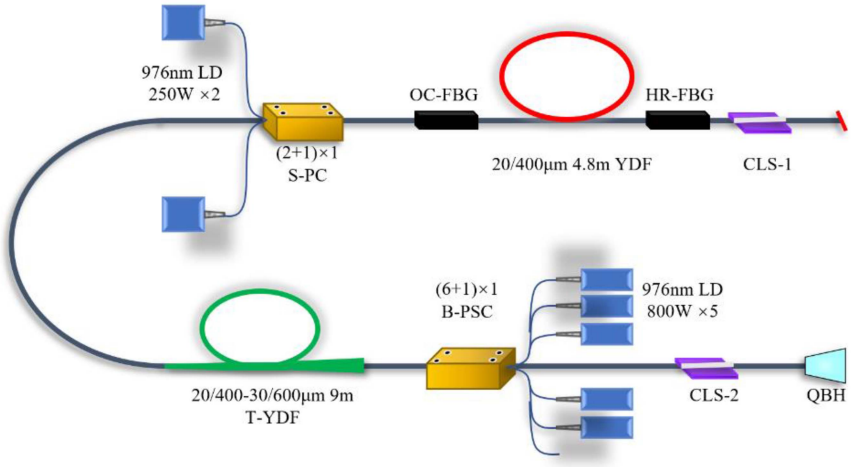

Fig. 1. Experimental setup of the counter-pumped fiber laser amplifier (CLS: cladding light stripper, HR-FBG: highly-reflected fiber Bragg grating, OC-FBG: output-coupling fiber Bragg grating, T-YDF: Tapered Yb-doped fiber, S-PC: side-pump combiner, B-PSC: backward-pump/signal combiner, QBH: quartz block head).

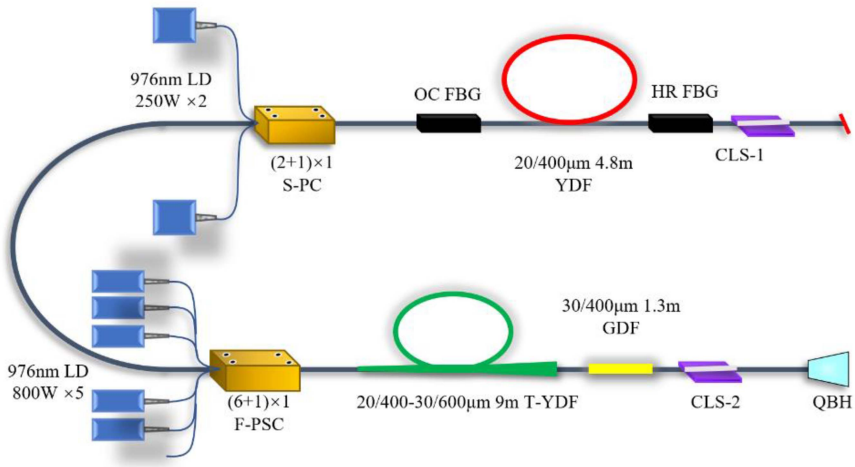

Fig. 2. Experimental setup of the co-pumped fiber laser amplifier (CLS: cladding light stripper, HR-FBG: highly-reflected fiber Bragg grating, OC-FBG: output-coupling fiber Bragg grating, T-YDF: Tapered Yb-doped fiber, S-PC: side-pump combiner, F-PSC: forward-pump/signal combiner, QBH: quartz block head, GDF: Ge-doped fiber).

from the nonreciprocity of the tapered structure, the tapered fibers exhibit a good suppression in nonlinear effects. Moreover, fiber laser using tapered fibers will achieve high efficiency and high beam quality.

In this manuscript, we constructed a monolithic tapered fiber laser operating at 1050 nm, employing a T-YDF with a narrow end of ∼20/400 μm and a wide end of ∼30/600 μm. The output performance was experimentally investigated with respective co-pumping and counter-pumping configuration, especially on the aspects of the SRS and TMI. The results show that the tapered fiber amplifier has significant suppression on SRS and TMI in both pumping schemes. There is no ASE in the maximum power spectrum. An output power of 3 kW-level was obtained with a nearly single mode beam quality (M2∼1.20). This work provides an effective solution for short-wavelength fiber amplifiers design to achieve high output power and high beam quality.

II. Experimental Setup

The monolithic fiber amplifier system employing T-YDF in the counter-pump and co-pump configurations are shown in Figs. 1 and 2, respectively. The systems both consist of a side-pumped seed and a main laser amplifier. Two 250 W 976 nm laser diodes (LDs) are injected into the resonant cavity via a (2 + 1) × 1 side-pumped combiner (S-PC). The cavity is a linear cavity composed of a pair of fiber Bragg gratings (FBGs) operating at a central wavelength of ∼1050 nm. The core and cladding diameters of the FBG are 20 μm and 400 μm, respectively. The output-coupling fiber Bragg grating (OC-FBG) has a reflection of 9.7% and a 3 dB reflection bandwidth of ∼2.05 nm. The highly-reflected fiber Bragg grating (HR-FBG) has a reflection of ∼99% and a 3 dB reflection bandwidth of ∼4 nm. The broadband laser oscillator feature of the seed laser is beneficial to improve the SRS threshold [23], [24], [25]. The core and

cladding diameters of the YDF fiber are 20 μm and 400 μm, a core numerical aperture (NA) is 0.065, and the total YDF length is 4.8 m. The pump absorption coefficients of the YDF at the wavelengths of 915 nm is 0.39 dB/m. To ensure beam quality of the seed, YDF is coiled on a water-cooled plate with a bending diameter of ∼10 cm. HR-FBG is fused to cladding light stripper (CLS-1) to filter out the cladding light, while the tailed fiber of CLS-1 is 8° angle cleaved to avoid facet reflection.

The output fiber tail of the S-PC is directly connected to the amplifier gain fiber. The length of the T-YDF is 9 m with a NA of 0.065 and the pump absorption coefficients at the wavelengths of 915 nm is ∼0.5 dB/m. The T-YDF self-fabricated has a narrow end of ∼20/400 μm and a wide end of ∼30/600 μm. The length of narrow end and wide end are 4 m and 2 m, respectively. And the length of the core/cladding gradually changed area is ∼3 m. The active fiber is coiled on the water-cooled plate with an "8"-shaped fiber groove. The fiber groove has a minimum coiling diameter of 8.2 cm, a maximum coiling diameter of 13 cm. The bending diameter of the groove is chosen to filter out higher order modes (HOMs) generated through bend loss, which have been proved quite effective for mitigating the TMI [26]. Each pump/signal combiner has six multimode pump ports with core/cladding diameters of 220/242 μm and a core NA of 0.22. The signal ports of backward-pump/signal combiner (B-PSC) are 30/400 μm and 30/250 μm double-clad fibers; the signal ports of forward-pump/signal combiner (F-PSC) are 20/250 μm and 20/400 μm double-clad fibers. Five LD modules used for both forward pump power and backward pump power, where each LD module emits at a stabilized wavelength of 976 nm and can launch a maximum power of ∼800 W. The unoccupied port of the pump/signal combiner is angle cleaved to remove the reflected light. In addition, in the co-pump experiments, a length of 1.3-m-long Ge-doped fiber (GDF) with core/cladding diameter of 30/400 μm is spliced to deliver the signal power and ensure the same conditions with the counter-pump. A home-made CLS (CLS-2) is utilized on the passive fiber to strip the unwanted cladding light and residual pump light. The length of home-made quartz block holder (QBH) is 1.5 m with core/cladding diameter of 30/400 μm. All components in the experiment are placed on the water-cooled plates for efficient thermal management and to ensure the stability of high-power operation.

In the fiber amplifier system, output power, beam quality, time domain signal and optical spectrum of the laser are measured and recorded. The output power laser is measured by a power meter. The spectra and beam quality are tested by an optical spectrum analyzer and a beam quality analyzer. The temporal characteristics of the output laser are recorded by a photodetector with a bandwidth of 1 GHz to test the time-domain signal.

III. Experimental Results and Discussion

In the experiments, we investigated the performances of 1050 nm T-YDF fiber amplifier with both counter-pumping and co-pumping configurations, respectively. As limited by the available pump power, we can only conduct co-pump or counter-pump experiments individual. TMI threshold, SRS intensity and beam quality are mainly compared, which will reflect the advantages of T-YDF.

The output power variations and corresponding optical-to-optical efficiency of two configurations are shown in Fig. 3(a) and (b). The output power increases with the pump power at a slope efficiency of ∼85.1% for the counter-pump and ∼86.4% for the co-pump. The fiber amplifier structure has influence in efficiency. Firstly, as we know, there are no FBGs with only about 90% of power can be output in the laser oscillator. Compared to fiber laser oscillator, fiber amplifier has higher efficiency. Secondly, we used pump LDs with stabilized wavelength at 976 nm, which can help the YDF to complete absorption of the pump power. The fiber amplifier we investigated is pump-sharing structure, there is no CLS between the seed laser and amplifier stage [9]. In the conventional amplifier structure, the residual pump light in amplifier stage cannot be utilized by seed. But in this pump-sharing structure, when the pump light of amplifier stage is not completely absorbed by gain fiber, it can be pumped into the seed stage through S-PC. Backward residual pump light increases the power of seed, further enhancing the output power of amplifier. It should be noted that the initial seed power is consistent for both pump methods. Another factor for the high efficiency is the application of T-YDF. The gradually-varying tapered region suppresses the generation of HOMs, thus few HOMs power leaks into the cladding [13].

In order to validate the onset of TMI, the temporal signals of the output laser were measured through a photodetector. Fig. 4(a), (b) show the temporal signals and corresponding Fourier spectra around the appearance of TMI under the counter-pump scheme. Fig. 4(c), (d) show the temporal signals and corresponding Fourier spectra around the appearance of TMI under the co-pump scheme. In counter-pump configuration, when the pump power is ∼3326 W and the output power is ∼2969 W, the temporal signal fluctuation is not obvious in the time range of 0–100 ms. But the frequency domain fluctuation is already observed in the range of 0–5 kHz. When the pump power is ∼3421 W and the output power is ∼3039 W, the signal fluctuation can be clearly seen in both the temporal signals and the Fourier spectra in Fig. 4(b), which are the typical TMI characteristics [27]. For co-pump, when the pump power is ∼2908 W and the output power is ∼2689 W, temporal signal fluctuations and corresponding frequency domain fluctuations are not obvious. When the pump power is ∼3122 W and the output power is ∼2818 W, the fluctuation frequency components distribute in the range of 0∼3 kHz. With increasing the pump power, the output power and efficiency decreased significantly, as shown in Fig. 4(d). When TMI occurs, FM transfer to HOMs. The HOMs have a higher bending loss and those lights were striped by the CLS, therefore, the output power seems to be decreased in Fig. 3(b).

The standard deviations (STD) of the recorded temporal signals and the beam quality of output laser were respectively studied for ensuring TMI thresholds. Fig. 5(a) shows the STD of the T-YDF fiber amplifier under co-pump and counter-pump schemes. The threshold of TMI can be defined with the abruptly raise of STD [27], [28], [29]. Applying this definition, in the T-YDF fiber amplifier, the TMI thresholds of co-pump and

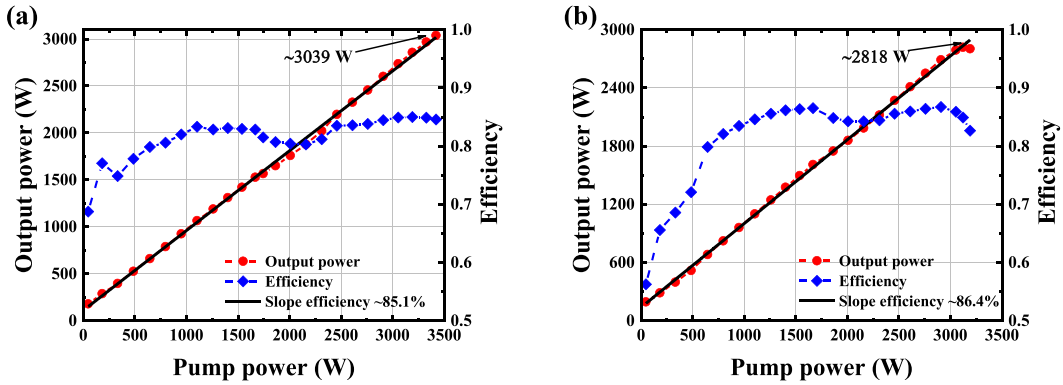

Fig. 3. The output power characteristics and corresponding optical-to-optical efficiency of the fiber amplifier. (a) In counter-pump scheme. (b) In co-pump scheme.

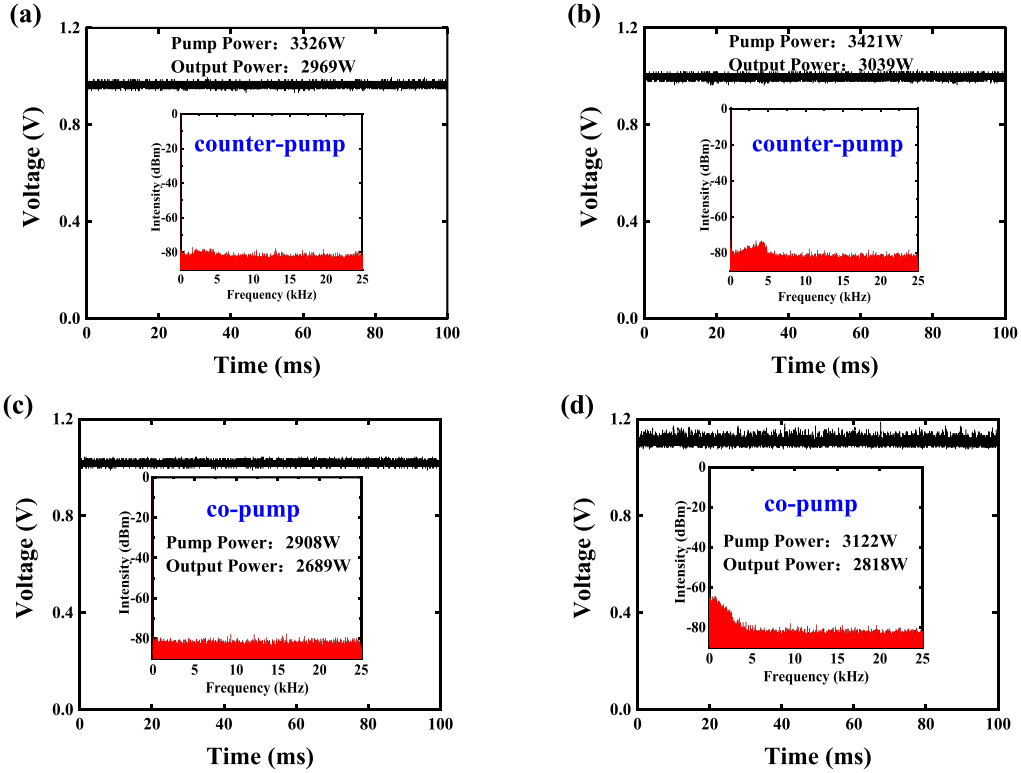

Fig. 4. Time domain signals and Fourier spectra in the frequency domain. (a) and (b) around the TMI threshold in counter-pump scheme. (c) and (d) around the TMI threshold in co-pump scheme.

counter-pump schemes are respective around 2818 W and 3122 W. However, the TMI threshold of the fiber amplifier needs to study the evolution of beam quality. The evolution of the laser spot shapes and the beam quality factor M^2 at different powers with increasing output power for the co-pump and counter-pump scheme is depicted in Fig. 5(b). In counter-pump, when the output power increases from ∼3039 W to ∼3211 W, the beam quality of output laser also degrades from 1.53 to 1.66 as shown in Fig. 5(b). In co-pump, the beam quality factor M^2 growth is relatively slow and has been below 1.20. It can be seen from the Fig. 5(a) that the change of STD raised in co-pump and counter-pump is different. The difference in beam quality can prove the change of STD. The worse beam quality in counter-pump indicates that the coupling between the fundamental mode (FM) and the HOMs already exists in the initial modes. When the TMI occurs, the STD will not raise abruptly. From the signal fluctuations in temporal and frequency domains and the degradation of the beam quality, it can be inferred that the TMI threshold in counter-pump is ∼3039 W. The beam quality in co-pump is always nearly single mode, so the STD raise abruptly with the TMI occurs. But from the signal fluctuation and the power roll-over in the co-pump, which implies the occurrence of TMI effect, it can also be inferred that the TMI threshold for co-pump is 2818 W.

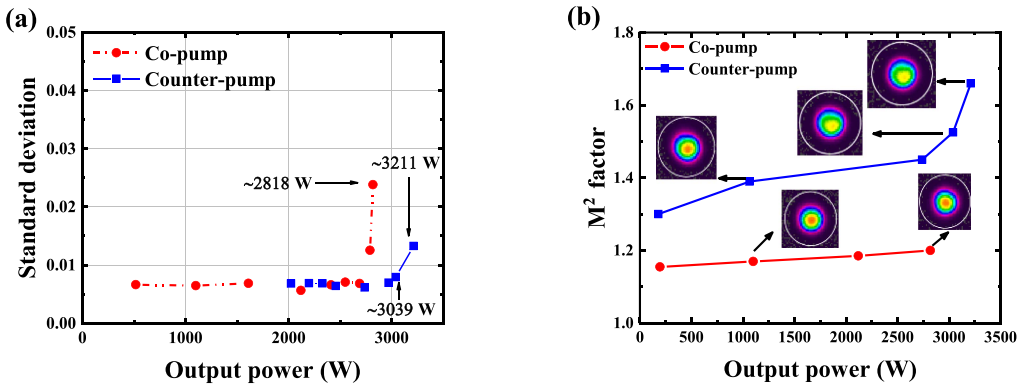

Fig. 5. (a) The STD of the T-YDF fiber amplifier under co-pump and counter-pump schemes. (b) The beam quality evolution during the power scaling of both fiber amplifiers.

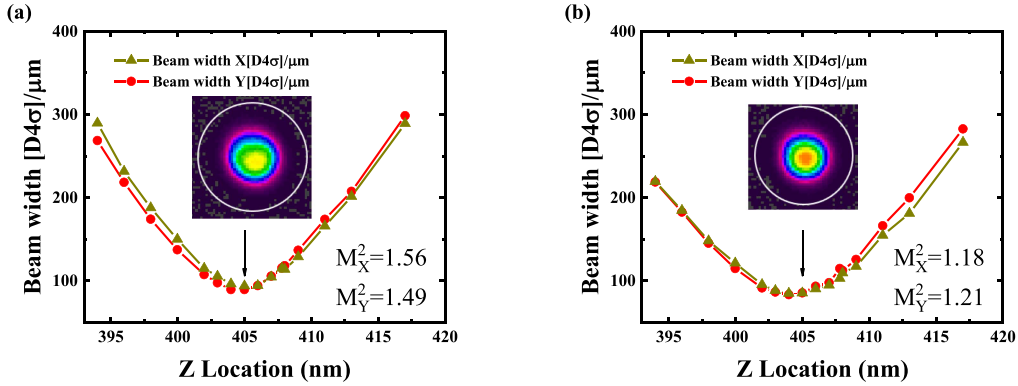

Fig. 6. Output laser beam quality at the TMI threshold. (a) In counter-pump scheme. (b) In co-pump scheme.

From the comparison results, the fiber amplifier built by T-YDF has a higher TMI threshold for counter-pump than co-pump. In co-pump, the pump light enters from the narrow end and the HOMs component in the core gradually strengthens in the total mode as the pump power increases. Conversely, pump light is injected from the wide end of the gain fiber in counter-pump, which is opposite to the direction of signal light transmission. The difference in the pump light injection direction leads to a different pump power distribution in the fiber, which in turn enhances the gain saturation effect and makes the TMI threshold higher for counter-pump than co-pump. On the other hand, the phenomenon of core laser leakage also exists in co-pump. When the power reaches around the TMI threshold, the HOMs leak into the inner cladding, resulting in a decrease in output power. Therefore, there is a drop of output power and efficiency after the TMI threshold in Fig. 3(b).

The beam quality at the TMI threshold for counter-pump and co-pump are shown in (a) and (b) of Fig. 6, respectively. The inset is the beam profile at the beam waist. The average beam quality factor is ∼1.53 and ∼1.20, respectively. The beam quality is better in co-pump than counter-pump. From the beam quality of the initial seed output, it can be seen that the fusion process in counter-pump is not as good as co-pump. The average beam quality factor of the seed is 1.30 and 1.18 in counter-pump and co-pump, respectively. It means that more HOMs are introduced into the amplifier stage in counter-pump than co-pump. With the pump power increasing, the HOMs are also amplified. The pump light enters from a small circle with a bending diameter of 8.2 cm on the runway in co-pump scheme. The HOMs generated at the front of the T-YDF are filtered out by bending loss. In counter-pump, the pump light enters from the large circle with a bending diameter of 13 cm on the runway. The HOMs generated at the rear of the fiber is less filtered out through bending loss. More HOMs are output with the signal light and reduce the beam quality, which is also the phenomenon that the beam quality of the counter-pump degrades rapidly as shown in Fig. 5(b). However, it can be demonstrated that the type of 20/400–30/600 T-YDF can achieve near single mode output by handling the fusion process.

The optical spectrum at the highest output power of counter-pump and co-pump are shown in Fig. 7(a) and (b). In counter-pump, the suppression ratio of SRS is ∼46.6 dB at the output power of 3039 W. The central wavelength is 1049.74 nm with a full width at half maximum (FWHM) of 3.0 nm, and there is a tiny spike on the left side of the central wavelength, which is inferred to four-wave mixing (FWM) [30], [31]. In co-pump, the suppression ratio of SRS is ∼33.2 dB at the output power of 2818 W. The central wavelength is 1050.27 nm with a FWHM of 1.02 nm. The difference of FWHM stems from degradation of beam quality caused by higher-order modes in counter-pump. The power distribution characteristics inside the T-YDF are obviously different for two pump schemes. The power distribution

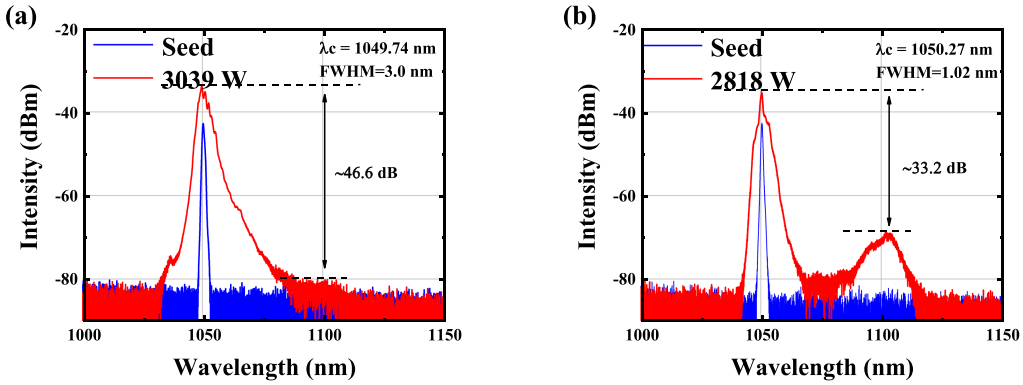

Fig. 7. Optical spectrum at the TMI threshold. (a) In counter-pump scheme. (b) In co-pump scheme.

inside the Yb-doped fiber is similar to the exponential pattern in the counter-pump direction and the logarithmic pattern in co-pump. The SRS effect is higher for the counter-pump than for the co-pump. The central wavelength of SRS in the spectra under both pump modes is ∼1100 nm, and the SRS intensity is acceptable for both pump modes. From the two spectra in Fig. 7, it can be seen that T-YDF are significantly superior for SRS suppression in short-wavelength fiber amplifiers [31]. The size of the tapered fiber we used is 20/400–30/600, the ratio of core diameter to cladding diameter (referred to as core-to-cladding ratio) remains constant along the length of the fiber. The filling factor of pump light does not change with length. The absorption coefficient of the tapered fiber at 915 nm is almost constantly 0.5 dB/m. In the 20/400 segment of tapered fiber, the SRS intensity increases with the fiber length. While in the 30/600 segment of single tapered fiber, the Raman gain coefficient decreases due to the increase of core and inner cladding size. The corresponding SRS intensity also decreases because of the LMA. The SRS suppression ratio in the co-pump and counter-pump scheme is about ∼33.2 dB at ∼3039 W and ∼46.6 dB at ∼2818 W, respectively. Thus, T-YDF has significant advantages in suppressing nonlinear effects such as SRS in short-wavelength fiber lasers.

IV. Conclusion

In summary, we have demonstrated a high power monolithic tapered fiber laser emitting at central wavelength of 1050 nm based on a T-YDF. The laser performances in counter-pump and co-pump configurations are studied, respectively. The TMI threshold is ∼3039 W with a slope efficiency of 85.05% in counter-pump and the average beam quality factor is 1.53. The TMI threshold is ∼2818 W with a slope efficiency of 86.43% in co-pump and the average beam quality factor is 1.20. In counter-pump and co-pump configurations, the suppression ratio of SRS is ∼46.6 dB and ∼33.2 dB. A near-single-mode beam quality (M2∼1.20) is obtained at output power of 3 kW-level. And the beam quality indicates that the 30/600 μm fiber is capable of near single-mode output by handling the fusion process. All these results show the advantages of single T-YDF in suppressing nonlinear effects, achieving high efficiency and high beam quality. T-YDF is helpful for amplifying of shorter wavelengths fiber lasers. From the experimental results, we believe that the fiber amplifier can achieve higher power and higher efficiency near-diffraction-limited output emitting at 1050 nm based on T-YDF.

Acknowledgment

The authors would like to thank Lingfa Zeng, Xiaoyong Xu, Siliu Liu, Pengfei Zhong and Tao Song for technical supporting during the experiments.

References

[1] S. J. Augst, J. K. Ranka, T. Y. Fan, and A. Sanchez, "Beam combining of ytterbium fiber amplifiers (Invited)," *J. Opt. Soc. Amer. B*, vol. 24, no. 8, pp. 1707–1715, 2007, doi: 10.1364/JOSAB.24.001707.

[2] T. Y. Fan, "Laser beam combining for high-power, high-radiance sources," *IEEE J. Sel. Topics Quantum Electron.*, vol. vol. 11, no. 3, pp. 567–577, May/Jun. 2005, doi: 10.1109/JSTQE.2005.850241.

[3] C. Fan et al., "10 kW-level spectral beam combination of two high power broad-linewidth fiber lasers by means of edge filters," *Opt. Exp.*, vol. 25, no. 26, pp. 32783–32791, 2017, doi: 10.1364/OE.25.032783.

[4] P. Ma, M. Jiang, X. Wang, Y. Ma, P. Zhou, and Z. Liu, "Hybrid beam combination by active phasing and bandwidth-controlled dichromatic mirror," *IEEE Photon. Technol. Lett.*, vol. 27, no. 19, pp. 2099–2102, Oct. 2015, doi: 10.1109/LPT.2015.2453356.

[5] N. A. Naderi et al., "High-efficiency, kilowatt 1034 nm all-fiber amplifier operating at 11pm linewidth," *Opt. Lett.*, vol. 41, no. 5, pp. 1018–1021, 2016, doi: 10.1364/OL.41.001018.

[6] P. Wu et al., "Optimization investigation for high-power 1034 nm all-fiber narrowband Yb-doped superfluorescent source," *Opt. Commun.*, vol. 445, pp. 187–192, 2019, doi: 10.1016/j.optcom.2019.04.033.

[7] Q. Chu et al., "3 kW high OSNR 1030 nm single-mode monolithic fiber amplifier with a 180 pm linewidth," *Opt. Lett.*, vol. 45, no. 23, pp. 6502–6505, 2020, doi: 10.1364/OL.405386.

[8] Y. Xu et al., "2.4 kW 1045 nm narrow-spectral-width monolithic single mode CW fiber laser by using an FBG-based MOPA configuration," *Appl. Opt.*, vol. 60, no. 13, pp. 3740–3746, 2021, doi: 10.1364/AO.420708.

[9] Y. Zheng et al., "3.1 kW 1050 nm narrow linewidth pumping-sharing oscillator-amplifier with an optical signal-to-noise ratio of 45.5 dB," *Opt. Exp.*, vol. 30, no. 8, pp. 12670–12683, 2022, doi: 10.1364/OE.456856.

[10] V. Filippov et al., "Double clad tapered fiber for high power applications," *Opt. Exp.*, vol. 16, no. 3, pp. 1929–1944, 2008, doi: 10.1364/OE.16.001929.

[11] Y. Ye et al., "Comparative study on transverse mode instability of fiber amplifiers based on long tapered fiber and conventional uniform fiber," *Laser Phys. Lett.*, vol. 16, no. 8, 2019, Art. no. 85109, doi: 10.1088/1612-202X/ab2acf.

[12] L. Zeng et al., "Near-single-mode 3 kW monolithic fiber oscillator based on a longitudinally spindle-shaped Yb-doped fiber," *Opt. Lett.*, vol. 45, no. 20, pp. 5792–5795, 2020, doi: 10.1364/OL.404893.

[13] C. Shi et al., "Theoretical study of mode evolution in active long tapered multimode fiber," *Opt. Exp.*, vol. 24, no. 17, pp. 19473–19490, 2016, doi: 10.1364/OE.24.019473.

[14] K. Bobkov et al., "Scaling of average power in sub-MW peak power Yb-doped tapered fiber picosecond pulse amplifiers," *Opt. Exp.*, vol. 29, no. 2, pp. 1722–1735, 2020, doi: 10.1364/OE.413528.
[15] C. Shi et al., "Theoretical study of stimulated Raman scattering in long tapered fiber amplifier," *Chin. Opt. Lett.*, vol. 15, no. 11, 2017, Art. no. 110605.
[16] V. Filippov et al., "600 W power scalable single transverse mode tapered double-clad fiber laser," *Opt. Exp.*, vol. 17, no. 3, pp. 1203–1214, 2009, doi: 10.1364/OE.17.001203.
[17] V. Filippov et al., "750-W double-clad ytterbium tapered fiber laser with nearly theoretically limited efficiency," *Proc. SPIE*, vol. 7580, pp. 314–326, 2010, doi: 10.1117/12.841239.
[18] A. Fedotov et al., "Ultra-large core birefringent Yb-doped tapered double clad fiber for high power amplifiers," *Opt. Exp.*, vol. 26, no. 6, pp. 6581–6592, 2018, doi: 10.1364/OE.26.006581.
[19] B. Yang et al., "High power monolithic tapered ytterbium-doped fiber laser oscillator," *Opt. Exp.*, vol. 27, no. 5, pp. 7585–7592, 2019, doi: 10.1364/OE.27.007585.
[20] Y. Ye et al., "Demonstration of constant-cladding tapered-core Yb-doped fiber for mitigating thermally-induced mode instability in high-power monolithic fiber amplifiers," *Opt. Exp.*, vol. 30, no. 14, pp. 24936–24947, 2022, doi: 10.1364/OE.462165.
[21] A. I. Trikshev et al., "A 160 W single-frequency laser based on an active tapered double-clad fiber amplifier," *Laser Phys. Lett.*, vol. 10, no. 6, 2013, Art. no. 065101, doi: 10.1088/1612-2011/10/6/065101.
[22] X. Wang et al., "Ytterbium doped variety core diameter fiber laser: Current situation and develop tendency," *Chin. J. Lasers.*, vol. 49, no. 21, 2022, Art. no. 2100001, doi: 10.3788/CJL202249.2100001.
[23] W. Liu et al., "Investigation of stimulated Raman scattering effect in high-power fiber amplifiers seeded by narrow-band filtered super fluorescent source," *Opt. Exp.*, vol. 24, no. 8, pp. 8708–8717, 2016, doi: 10.1364/OE.24.008708.
[24] Y. Ye et al., "Experimental study of SRS threshold dependence on the bandwidths of fiber Bragg gratings in co-pumped and counter-pumped fiber laser oscillator," *J. Opt.*, vol. 21, no. 2, 2019, Art. no. 025801, doi: 10.1088/2040-8986/aafa65.
[25] W. Liu et al., "General analysis of SRS-limited high-power fiber lasers and design strategy," *Opt. Exp.*, vol. 24, no. 23, pp. 26715–26721, 2016, doi: 10.1364/OE.24.026715.
[26] H. Lin et al., "3.7 kW monolithic narrow linewidth single mode fiber laser through simultaneously suppressing nonlinear effects and mode instability," *Opt. Exp.*, vol. 27, no. 7, pp. 9716–9724, 2019, doi: 10.1364/OE.27.009716.
[27] H. J. Otto et al., "Temporal dynamics of mode instabilities in high-power fiber lasers and amplifiers," *Opt. Exp.*, vol. 20, no. 14, pp. 15710–15722, 2012, doi: 10.1364/OE.20.015710.
[28] F. Beier et al., "Experimental investigations on the TMI thresholds of low-NA Yb-doped single-mode fibers," *Opt. Lett.*, vol. 43, no. 6, pp. 1291–1294, 2018, doi: 10.1364/OL.43.001291.
[29] M. M. Johansen et al., "Frequency resolved transverse mode instability in rod fiber amplifiers," *Opt. Exp.*, vol. 21, no. 19, pp. 21847–21856, 2013, doi: 10.1364/OE.21.021847.
[30] Y. Zhang, J. Ye, X. Ma, J. Xu, T. Yao, and P. Zhou, "Efficient lasing through Raman-assisted four-wave mixing with intrinsic weak spectral broadening characteristics," *J. Lightw. Technol.*, vol. 40, no. 4, pp. 1173–1180, Feb. 2022, doi: 10.1109/JLT.2021.3126009.
[31] Y. Feng et al., "Spectral broadening in narrow linewidth, continuous-wave high power fiber amplifiers," *Opt. Commun.*, vol. 403, pp. 155–161, 2017, doi: 10.1016/j.optcom.2017.07.005.